

DNN-PolSAR: Urban Image Segmentation and Classification using Polarimetric SAR based on DNNs



Soumyadip Sarkar, Farhan Hai Khan, Shobhit Kumar, Tamesh Halder, Dipjyoti Paul, Debashish Chakravarty

Abstract. Synthetic Aperture Radar (SAR) image segmentation and classification is a popular technique for learning and detection of objects such as buildings, trees, monuments, crops water-bodies, hills, etc. SAR technique is being used for urban development and city-planning, building control of municipal objects, searching best locations, detection of changes in the existing systems, etc. using polarimetry based on Deep Neural Networks. In this paper, we proposed a technique for Urban Image Segmentation and Classification using Polarimetric SAR based on Deep Neural Networks (DNN-PolSAR). In our proposed DNN-PolSAR technique, we use Mask-RCNN, LinkNet, FPN, and PSP-Net as model architectures, whereas ResNet50, ResNet101, ResNet152, and VGG-19 are used as backbone networks. We first apply polarimetric decomposition on airborne Uninhabited Aerial Vehicle Synthetic Aperture (UAVSAR) images of urban areas and then the decomposed images are fed to DNNs for segmentation and classification. We then simulate DNN-PolSAR considering different hyper-parameters and compare the obtained scores of hyper-parameters against used model architectures and backbone networks. In comparison, it is found that DNN-PolSAR based on FPN model with ResNet152 performed the best for segmentation and classification. The mean Average Precision (mAP) score of the DNN-PolSAR based on FPN with a pixel accuracy of 90.9% is 0.823, which outperforms other Deep Learning models.

Keywords: Polarimetric SAR, FPN, PSPNet, Mask-RCNN, LinkNet, Image Segmentation.

I. INTRODUCTION

Segmentation and classification of an image is a process of splitting and categorizing the image into different parts based on the predefined category of objects. In this process, each pixel in an image is categorized based on the predefined labels of objects.

Manuscript received on 12 April 2024 | Revised Manuscript received on 11 May 2024 | Manuscript Accepted on 15 May 2024 | Manuscript published on 30 May 2024.

*Correspondence Author(s)

Soumyadip Sarkar, Institute of Engineering & Management, Kolkata, India. Email: soumya997.sarkar@gmail.com

Farhan Hai Khan, Institute of Engineering & Management, Kolkata, India. Email: njrfarhandasilva10@gmail.com

Shobhit Kumar, Institute of Engineering & Management, Kolkata, India. Email: shobhit.course@gmail.com

Tamesh Halder*, Department of Mining Engineering, Indian Institute of Technology, Kharagpur, India. E-mail: haldertamesh@iitkgp.ac.in, ORCID ID: [0000-0002-9363-1471](https://orcid.org/0000-0002-9363-1471)

Dipjyoti Paul, Department of Computer Science, University of Crete, Heraklion, Crete, Greece. Email: dipjyoti92@gmail.com

Debashish Chakravarty, Department of Mining Engineering, Indian Institute of Technology, Kharagpur, India. Email: profdcitkgp@gmail.com

© The Authors. Published by Blue Eyes Intelligence Engineering and Sciences Publication (BEIESP). This is an open access article under the CC-BY-NC-ND license <http://creativecommons.org/licenses/by-nc-nd/4.0/>

Image segmentation has historically been used primarily for recognizing scenes in which similar objects can be placed more accurately. However, recently image segmentation is being used in different fields such as medical imaging, autonomous driving, etc. very successfully. Therefore, image segmentation can also be used for satellite image and Polarimetric SAR (PolSAR) of urban cover areas for categorization and analysis [1],[2].

PolSAR is a very popular technique in remote sensing and it is used in wide ranges of applications namely segregation and classification in GIS, remote sensing, etc. It is also used for mapping of areas such as forest, vegetation, urbanized areas, etc. Data generated from PolSAR provides SAR resolutions, which help to understand images in forms of scattering components such as surface scattering, volume scattering, helix scattering, double-bounce scattering, and wire scattering. Based on these scattering components, PolSAR helps to understand classification of objects. For example, it is seen that PolSAR generates more prominent helix and double-bounce scattering components for images of urban areas [3]–[5][41][42][43]. Here in this work, we consider double-bounce scattering and helix scattering components for classification of objects in images of urban areas. However, with growth of urbanization and increasing population in urban areas, tracking, studying and analysis of the urban cover areas have become very essential, particularly in terms of locating and classifying objects such as buildings, crops water-bodies and hills. So, accurate locating and classification of different objects using images of urban areas is important for designing quick and reliable solutions [6]. But, urban image segmentation and classification is a very challenging task even using SAR polarimetry. This is because urban cover relatively shows small part of total surface. Fortunately, a huge collections of satellite imagery datasets is available freely which can be used for image segmentation and classification of urban cover areas.

Image segmentation and classification of urban cover areas using PolSAR is very difficult task due to urban structures, whose orientation is not in line of sight (LoS) of the radar. However, recognition of such areas is important for a number of reasons such as disaster relief, urban planning, and environmental monitoring. But, it is not possible to feed the scattering of images of urban covers areas taken using the Uninhabited Aerial Vehicle Synthetic Aperture Radar (UAVSAR) into a neural network.

This is because it is required to employ a set of decomposition of images in order to retrieve various information using scattering such as surface scattering, double bounce scattering, volume scattering, helix scattering, wire scattering, etc. It is also required to identify different areas such as grassland, urban areas, hills, etc. with different scattering information and components from the images, so the data obtained from scattering become significant. A scattering component allows us to determine what kind of area is captured in particular images. A grassland, for example, may have high values for surface scattering, while an urban area may have high values for both double bounce and helix scattering. With the application of these decomposition techniques to the UAVSAR raw scattering matrix elements, different areas tend to exhibit different characteristics, which can be used to perform image segmentation and classification. Based on the above mentioned principle, in this paper, we present a technique for Polarimetric SAR (PoSAR) image segmentation and classification of Radar Satellite Imagery of urban areas using Deep Neural Networks (DNNs) such as PSPNet, LinkNet, FPN, and Mask-RCNN based on different backbone networks such as such as Efficient-Net, DenseNet, MobileNet, Inception, ResNet, and VGG19 (discussed in Subsection 3.1). In our proposed technique, we first apply polarimetric decomposition on airborne UAVSAR images of urban areas and then the decomposed images are fed to DNNs for segmentation and classification. We simulate our proposed technique and accordingly obtain simulation results using different DNNs. The major contributions of this work are as follows:

We propose a technique consisting of models and backbone networks for urban classification and perform rigorous evaluation of all the machine learning classifiers in the field of Remote Sensing. We propose a technique to identify and detect buildings, grassland, hills from the PoSAR images.

- Presented and described the best and most effective Deep Learning methods for PoSAR image segmentation and classification.
- We obtain simulation results of our proposed technique with different backbone networks such as EfficientNet, DenseNet, MobileNet, Inception, ResNet, and VGG19.
- We carried out an extensive comparison and discussion of the current state-of-the-art models on the same datasets for segmentation and classifications of urban area covers.

The remainder of the paper is organized as follows. Section 2 presents Related Work in the area of satellite image segmentation and classification. In Section 3, we discuss the architectures and backbones of the models, which are used in our paper. An overview of the datasets used for training and validation is discussed in Section 4. In Section 5, results of experimentation based on different databases and discussion on the results are presented. Finally, we concluded our paper in Section 6.

II. RELATED WORKS

Segmentation of PoSAR images of urban cover areas poses unique challenges such as partial visibility of surfaces, different scattering, etc. However, only good thing is that area structure of the these images are well defined. But,

design and development of algorithms for analysis and classifications of such as images requires focused research for opening possibilities for the application of Remote Sensing in various fields. In view of this, A number of works has been proposed for image analysis and classification using semantic segmentation. In this section, we briefly present and discuss some of the advancements in classification approaches for PoSAR as well some of the examples where architectures from a different area of study has been successfully applied in remote sensing. A recent study conducted by De et al [7] to build a Deep Learning based novel technique for classification of urban areas. The information in the augmented dataset used in this work is trans-formed using a stacked auto-encoder, before feeding it to a neural network for classification. This technique achieved an accuracy of 91.3%, which was an enhancement in performance as compared to the techniques present at that time. In, [8] Cui et al proposed an architecture comprising Dense Attention Pyramid Network (DAPN), Region Proposal Network (RPN) and a detection network for multi-scale ship detection in SAR images. Here, DAPN was used to extract multi-scale fused features for generating and detecting to use in the subsequent iterations of the technique. The top-down densely connected networks are used to get concatenated feature maps of lower layers. The proposed method provided an accuracy of 89.8%, which was 11% higher than the previous models on the SAR ship detection data set (SSSD). DAPN was also 20% more than the faster R-CNN [9]. They also showed that the top-down pyramid structure with attention is very effective in obtaining the feature maps which contained more spatial and semantic information. Recently, Mohanty et al presented applications of Mask-RCNN [10] on the segmentation and detection of building on Google Maps Satellite Imagery Data. Authors found the results to be impressive with a final loss value of 0.15 for the instance image segmentation model. Wang et al. explored the problems in the classification of PoSAR images due to the presence of nonlinear data. This study proposed a kernel sparse representation based classification approach. This kernel function technique solves the problems caused by the nonlinear features. This helps in attaining more accurate results in the task of classification. This study used an Airborne SAR dataset from San Francisco, United States of America. In, [12] Femin et. al. proposed an approach for detecting buildings using CNN from satellite images. In this work, different building footprints from the images were identified using CNN method. The proposed work was also detected different shapes and colors.

The detection accuracy by this approach for building was found to be 83%. On the other hand, Wang et al. introduced a deep feature extraction approach in, [13] where multilevel polarimetric feature vector is extracted using a PAO PTD CNN. The authors extracted superpixels using simple linear iterative clustering (SLIC) from the feature vector for classification map. Finally, the result is obtained combining the superpixel map and the deep feature classification vector with Kappa Score of 0.86. The authors of [14] mentioned that the semantic segmentation can also be implemented for high-resolution.

PolSAR images using neural network architecture such as MP-ResNet, which contains three concurrent semantic embedding branches and uses a multi-scale feature fusion design in de-coder to use each encoding branch.

The authors noticed that MP-ResNet improves the aggregation of context information compared to baseline Fully Convolution Network (FCN). The suggested method based on MP-ResNet surpasses numerous state-of-the-art methods in all accuracy with a mean F1 of 92.25% and IoU of 89.60% in classification using the Gaofen Dataset. Zhao et. al. showed in [15] that segmentation can also be achieved using edge information based on spectral graph partitioning. Here, the authors defined segmentation as a three-part process namely edge information extraction, edge-based similarity matrix analysis, and normalised cut. This method overcame the pepper-salt phenomenon along with much more complete and the boundaries of the segments. The method of [16] by Ouahabi et. al. aimed to improve the segmentation efficiency without compromising the accuracy using Fully Convolution dense Dilated Network model. Here, the authors found that the Low resolution and contrast, shadow interference as well as differences in size and position of the abnormal tissue are the challenges that hinder the process of obtaining the segmentation of ultrasound images. Yuanyuan et al. in their work [17] explore how different classification algorithms are affected by the choice of polarimetric parameters such as Alpha, HAA, T11, Shannon entropy, VanZyl3 Vol, Neuman delta mod, Barnes2 T33, Barnes1 T33, and entropy.

III. BACKBONE NETWORK AND MODEL ARCHITECTURE

A. Backbone Networks

A backbone network is mainly used to extract network feature for classification of objects. Here, in this paper we have used ResNet152, [18] ResNet101, [19] ResNet50, and VGG-19 [20] backbone networks for features extraction from images.

B. Model Architectures

In this Subsection, we explain model architectures such as M-RCNN, PSPNet, FPN, and LinkNet used for classification in our work. The model architectures classify the extracted features using the base model from the deep neural backbone networks discussed in 3.1.

C. MR-CNN

The M-RCNN [21] was developed as an extension to the Faster-RCNN [9] which has been widely used so far for various object detection purposes. The F-RCNN/M-RCNN as output yields an object's label along with the object's bounding box. F-RCNN uses a feature extractor block that extracts the features from the image. These features are then used to train the bounding box regressor and the classifier. The M-RCNN as the name extends F-RCNN by training a binary mask in parallel with the bounding box regressor and object classifier. The first stage of the Mask-RCNN (like the F-RCNN) is the Region Proposal Network (RPN). Each bounding box is paired with an objectness score that denotes the probability score of the object. The second stage of the M-RCNN is called the head of the network. In F-RCNN this head is generally a stack of convolution layers and a

dense layer for bounding box regression. M-RCNN in parallel to this bounding box learning algorithm uses a stack of convolution layers for Mask representation. This parallel task makes it theoretically faster and more accurate than other segmentation models.

D. Feature Pyramid Network (FPN)

A FPN is a fully convolutional feature extractor that takes a single-scale image of any size as input and produces correspondingly sized feature maps at several layers. [22] The model comprises two distinctive parts such as a conventional convolutional network (like VGG19 or ResNet50) that acts as a feature extractor and a deconvolutional network with compatible feature sizes. However, there is a crucial difference between these two parts: the convolutional network goes from bottom to top whereas the flow in the deconvolutional network goes from top to down. The blocks in the convolutional network are connected in the deconvolutional network by linear multiplication. The output of blocks in the deconvolutional layer are connected to individual convolution layers which are not directly connected. These layers are transformed into a stack of layers. This dataset undergoes some upsampling and activation to give us an image map.

E. LinkNet

The LinkNet is a lightweight network architecture designed for performing segmentation tasks with a special focus on processing time [23]. Instead of a typical auto-encoder style segmentation model where the spatial semantics are first extracted using encoder blocks and then the decoder uses this spatial information for spatial categorization. This method has a certain downside in terms of both computation and accuracy. The pooling and strided convolution used in encoders may result in some loss of spatial information. So instead, the LinkNet algorithm uses skip connections from one encoder block to the corresponding block to prevent the loss of information at each stage. This idea of semantic information preservation is very similar to an U-Net except in this case the results of the encoder are added to the results of the corresponding decoder block instead of performing feature concatenation. For experimentation, we will be using the model proposed in the original LinkNet paper. The model uses four encoder blocks and four corresponding decoder blocks. There are two special blocks of fully convolutional neural networks at the beginning and end of the network to preserve the dimensions of the image.

a. Pyramid Scene Parsing Network (PSPNet)

The PSPNet of [24] is a model used for semantic segmentation. Its specialty is that it uses a pyramid parsing module. Different region-based context aggregation is used by this module to exploit global context information.

The final predictions are made more reliable due to the presence of local and global clues together. Given an input image, the feature map can be extracted using a pre-trained CNN, using a dilated network strategy.

The final size of the feature map is reduced to 1/8th of the input image. A pyramid pooling module is then applied on the top of the map, for gathering context information. A four-level pyramid is used where the pooling kernels cover the whole, half of, and small parts of the image.

The results from the pooling kernels are then concatenated to form a global prior. In the next step this prior is concatenated to the original feature map. The obtained result is finally passed through a stack of convolutional layers to generate the final prediction.

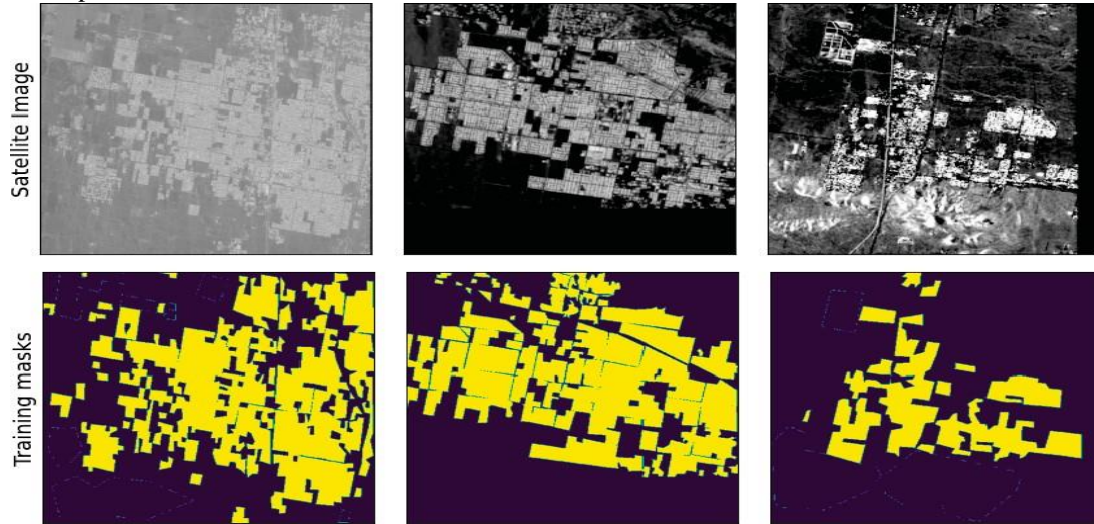


Fig 1: Sample Datasets and their Corresponding Masks for Urban Areas

We have mentioned in Section 1 that a huge collection of satellite imagery datasets of urban cover areas is readily available for image segmentation and classification. Therefore, in order to train our proposed algorithm, we have used PoSAR images of Lancaster, Palmdale and Rosamond city from airborne UAVSAR. However, we have considered only building classes for semantic and instance segmentation from these datasets using Deep Learning over various polarimetric decompositions. It is also to be mentioned that as similar of, [17] we have used different polarization parameters such as Alpha, HAAAlpha T11, Shannon entropy, VanZyl3 Vol, Neuman delta mod, Barnes2 T33, Barnes1 T33, and entropy to improve the classification accuracy in our proposed technique. We use PoSARPro v6.0 Software Suite [40] for decomposition results in our proposed work. In Table ??, we show all the decomposition methods and

IV. DATASETS AND USAGE IN PROPOSED TECHNIQUE

Datasets play an important and crucial role in any machine learning algorithms for segmentation and classification. In our proposed technique too datasets play major roles in segmentation of classification of images of urban cover areas.

corresponding polarimetric parameters those were applied on the datasets in our proposed technique. It is required to be mentioned that we also performed image augmentation using random rotation and image flipping to generate more data before passing them through the model. We generated 3 transformed images from each image with size of 1331 1101 3 for enhancing our datasets. The enhanced datasets are used for training based on PoSAR images of Lancaster, Palmdale, and Rosamond cities of USA. The reason of usage of datasets from different cities for increasing segmentation accuracy by introducing variance in the datasets. Detail of used datasets are given in Table 2. It can be seen from Table 2 that there are 71, 60, and 50 training datasets for Lancaster, Palmdale, and Rosamond respectively. But, we used 33, 64, and 17 test datasets for Lancaster, Palmdale, and Rosamond respectively.

Table 1 Shows Sample Datasets of Satellite Images (The Upper Parts of the Figure) as well as

Decomposition Method	Polarimetric Parameter		
Cloude [25]	Cloude T11	Cloude T22	Cloude T33
H/A/Alpha [26]	Entropy H/A/A T11	Anisotropy H/A/A T22	Shannon Entropy H/A/A T33
VanZyl3 [26]	VanZyl3 Vol	VanZyl3 Odd	VanZyl3 Dbl
Neuman [27]	Neuman delta mod	Neuman delta pha	Neuman tau
FreeMan2 [28]	FreeMan2 Vol	FreeMan2 Ground	
FreeMan [29]	FreeMan Vol	FreeMan Odd	Freeman Dbl
Huyen [30]	Huyen T11	Huyen T22	Huyen T33
Bhattacharya [31]	Frey Dbl	Frey Hlx	Frey Odd
Singh [32]	Singh 6SD1	Singh G4U2 Vol	Singh G4U2 Odd
Barnes1 [33]	Barnes1 T11	Barnes1 T22	Barnes2 T33
Barnes2 [33]	Barnes2 T11	Barnes2 T22	Barnes2 T33
Pauli [25]	Pauli a	Pauli b	Pauli c
Holm1 [34]	Holm1 T11	Holm1 T22	Holm1 T33
Holm2 [34]	Holm2 T11	Holm2 T22	Holm2 T33
Arri3 NNED [35]	Arii NNED Vol	Arii NNED Odd	Arii NNED Dbl
An Yang3 [36]	An Yang3 Vol	An Yang3 Odd	An Yang3 Dbl
An Yang4 [37]	An Yang4 Vol	An Yang4 Odd	An Yang4 Dbl
Yamaguchi3 [38]	Yamaguchi3 Vol	Yamaguchi3 Odd	Yamaguchi3 Dbl
Yamaguchi4 [39]	Yamaguchi3 Vol	Yamaguchi3 Odd	Yamaguchi3 Dbl

Table 2: Description of the Datasets

Location	Coordinates		Region/Country	Datasets	
	Latitude	Longitude		Train	Test
Lancaster	40.037° N	76.305° W	Pennsylvania, USA	71	33
Rosamond	34.8641° N	118.1634° W	Karen County, California, USA	60	64
Palmdale	34.3452° N	118.62° W	Los Angeles, California, USA	50	17

corresponding masks (the lower parts of the Figure) of the satellite images. From Figure 1, it can be seen that our proposed technique based on datasets correctly segmented and classified urban areas from the images. In the lower parts of the Figure 1, the yellow color masks represent the presence of urban areas for the given satellite images. Details of results with our proposed technique and discussion on the results are given in the following Section 6.2.

A. Proposed Technique

We employ Deep Neural Networks (DNNs) like PSPNet, LinkNet, FPN, and M-RCNN based on various backbone networks such as EfficientNet, DenseNet, MobileNet, Inception, ResNet, and VGG19 to segment and classify Radar Satellite Imagery of Urban Areas. The block diagram of the proposed technique is shown in Figure 2. In the proposed technique, first the polarimetric decomposition and Refined Lee filter are applied on the airborne UAVSAR images of urban areas. The decomposed images are then fed to DNNs along with respective backbone networks for segmentation and classification. From Figure 2, it can be seen that the FPN, PSP Net, and Link Net use three different backbone networks such as ResNet50, ResNet152, and VGG19, whereas M-RCNN uses ResNet50, ResNet101, and VGG19 as backbone networks.

B. Simulation Studies

In this Section, we present simulation results of our proposed technique and a discussion on the simulation results. It is to be mentioned that the main motivation of our work is to understand the learning capacity and rate of convergence of segmentation and classifications of images against the above mentioned architectures with different backbone networks. In order to do that we have considered four different model architectures as well as four different backbone networks to obtain unbiased results. We have used hyper-parameters such as *Intersection Over Union (IoU) score*, *Pixel Accuracy*, *F1 Score*, *Cohen’s Kappa Score*, *Area Under the Curve*, *Recall*, *Precision*, and *Mean Average Precision (mAP)* as performance metrics to obtain simulation results of learning capacity and rate of convergence by our proposed technique. We have also discussed these metrics to draw performance comparison of different architectures and backbone networks.

C. Simulation Environment

We have simulated our proposed technique using Python3 on a Kaggle, Colab notebook and R language in a computer with 64 GB RAM. Simulation is conducted using model architectures namely M-RCNN, FPN, LinkNet, PSPNet against the ResNet152, ResNet101, ResNet50, and VGG-19 backbone networks. However, we provided results of best performing backbone networks for each considered model architectures.

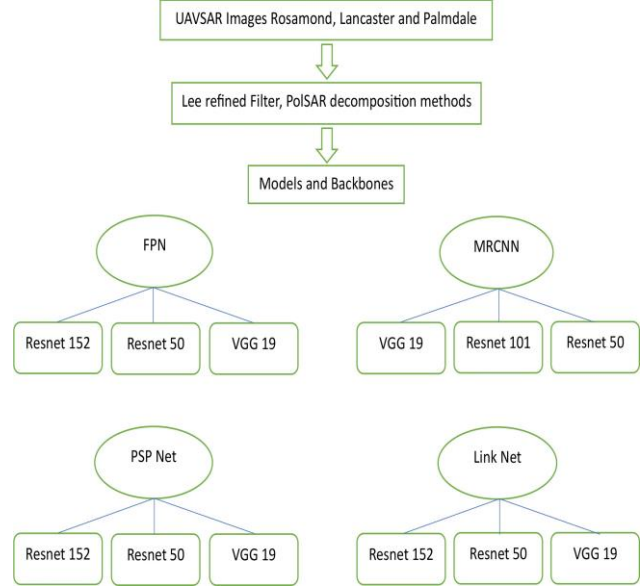


Fig 2: Block Diagram of Our Proposed Scheme

V. RESULTS AND DISCUSSION

In this section, we present simulation results and discussion. Simulation results presented considering popular hyper-parameters for used deep learning algorithms in our approach. Timely convergence of deep learning algorithms is crucial and very essential. So, we also presented and analysis of convergence of the used DL algorithm in the our work. In the last subsection of the section, a case study is also presented considering prediction accuracy of the urban images.

A. Numerical Results

In Table 3, we presented simulation results of Pixel Accuracy, Cohen’s Kappa Score, IoU Score, mean Average Precision, Area Under the Curve.

Recall, Precision, and F1 Score hyper-parameters for all the considered model architectures and backbone networks. From Table 3, it can be seen that Cohen’s Kappa Score and IoU Score for FPN with ResNet152 is highest compared to all other scores. It can also be seen from Table 3 that mAP, AuC and F1 Scores for FPN with ResNet152 and VGG19 are highest respectively. Therefore, it may be concluded that the FPN gives the best accuracy among all models proposed in this paper.

The high F1 score and AuC scores for the top three models confirm that the FPN architecture performs best among all other architectures. It gives pixel accuracy above 90% for three backbones, namely ResNet152, VGG-19, and ResNet50. On the other hand, it can be seen from Table 3 that the Pixel Accuracy of 91% for LinkNet with ResNet152 is highest. But the values of Recall and Precision are highest for LinkNet with ResNet50 and ResNet152 respectively.

Table 3: Pixel Accuracy, Cohen’s Kappa Score, IoU Score, mAP, AuC, Recall, Precision, and F1 score of all Considered Model Architectures and Backbone Networks

Model Architecture	Backbone Network	Pixel Accuracy	Cohen’s Kappa Score	IoU Score	mAP	AuC	Recall	Precision	F1 Score
FPN	ResNet152	0.909	0.806	0.799	0.823	0.965	0.917	0.850	0.882
	ResNet50	0.901	0.786	0.774	0.808	0.963	0.879	0.861	0.870
	VGG-19	0.909	0.805	0.796	0.817	0.968	0.928	0.843	0.884
MR-CNN	ResNet101	0.897	0.781	0.780	0.809	0.950	0.897	0.839	0.867
	ResNet50	0.638	0.057	0.069	0.394	0.634	0.075	0.647	0.134
	VGG-19	0.811	0.621	0.667	0.672	0.937	0.973	0.671	0.794
PSPNet	ResNet152	0.885	0.755	0.753	0.768	0.960	0.934	0.795	0.859
	ResNet50	0.895	0.771	0.758	0.784	0.961	0.896	0.835	0.865
	VGG-19	0.893	0.772	0.763	0.788	0.957	0.907	0.824	0.864
LinkNet	ResNet152	0.910	0.805	0.791	0.822	0.966	0.895	0.868	0.881
	ResNet50	0.464	0.127	0.419	0.419	0.618	1.000	0.411	0.583
	VGG-19	0.715	0.461	0.573	0.579	0.890	0.968	0.570	0.718

The pixel accuracy, cohen’s kappa, IoU score, AuC, Recall Precision, and F1 Score of MR- CNN with ResNet101 is better compared to other backbone networks. Based on these values of parameters, it can be inferred that the MR-CNN model architecture is the largest model used herein terms of the number of trainable parameters and consequently this architecture takes more time to train the system considering all used images than other considered model architectures.

Finally, the Pixel Accuracy with ResNet50 and Cohen’s Kappa Score and IoU Score with VGG19 for PSPNet are better compared to other two backbone networks. The values of AuC with ResNet50, Recall with ResNet152 Precision and F1 Score with ResNet50 are best. It can specifically be inferred about PSPNet that the PSPNet architecture performs well with VGG-19, ResNet50 and ResNet152 respectively as its backbone networks.

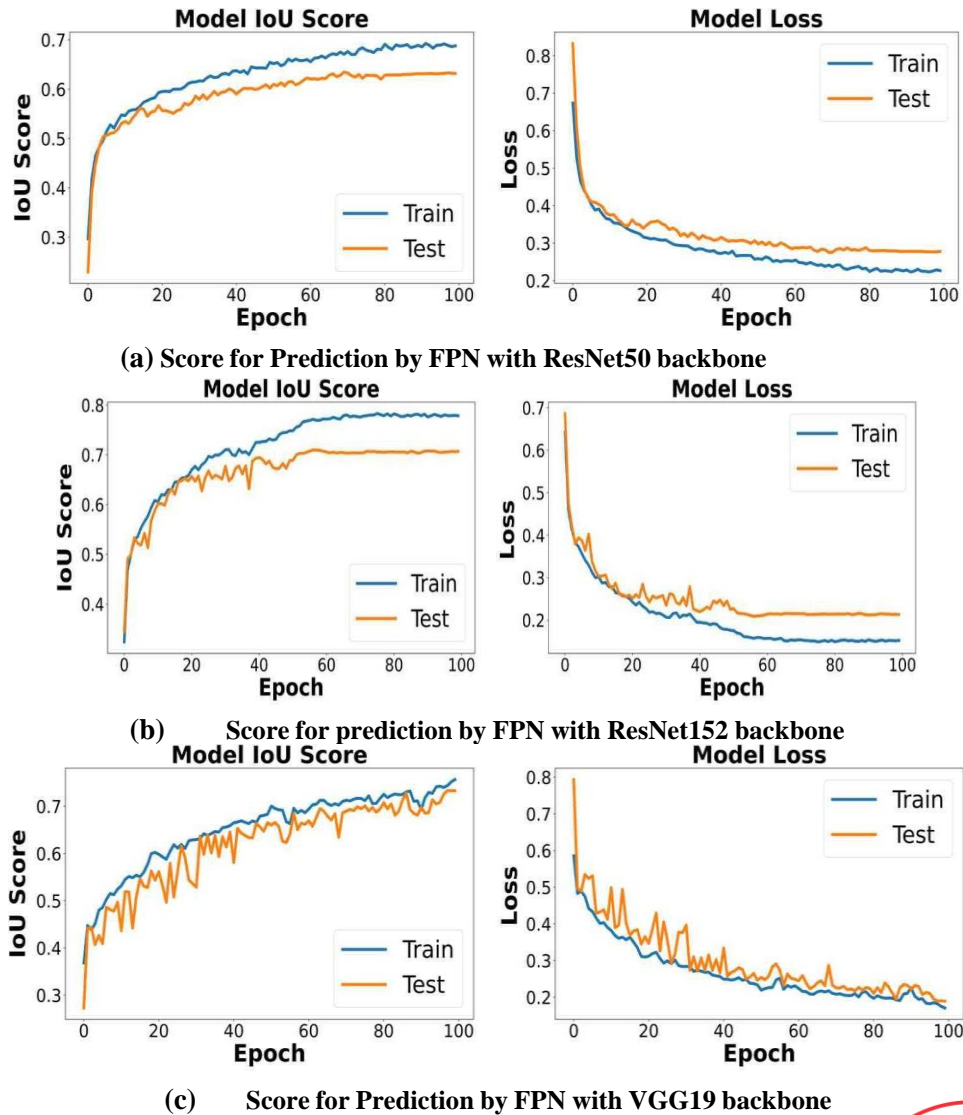
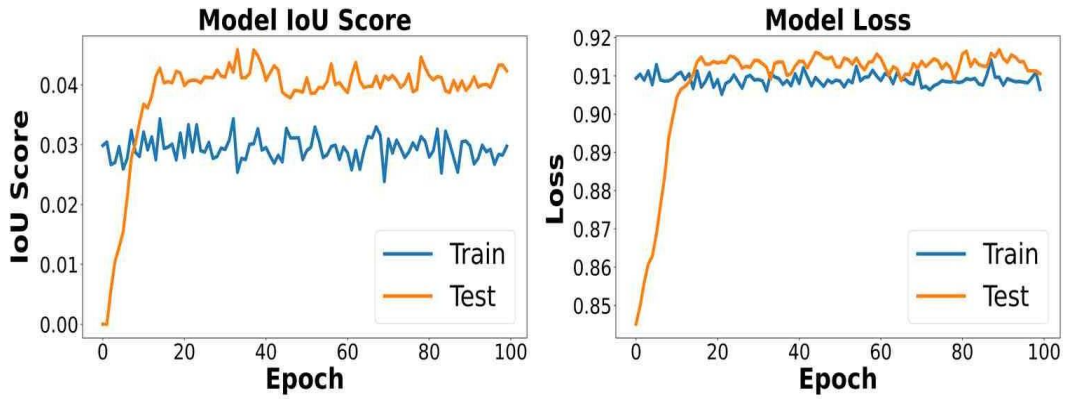
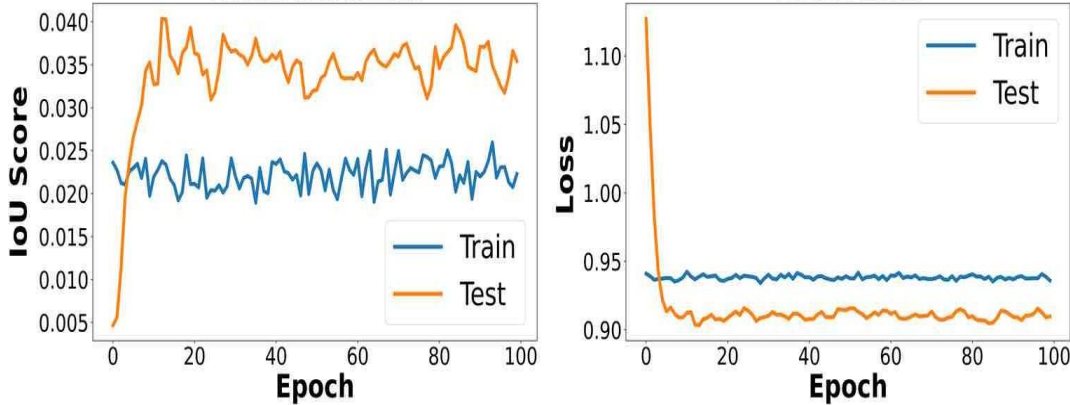


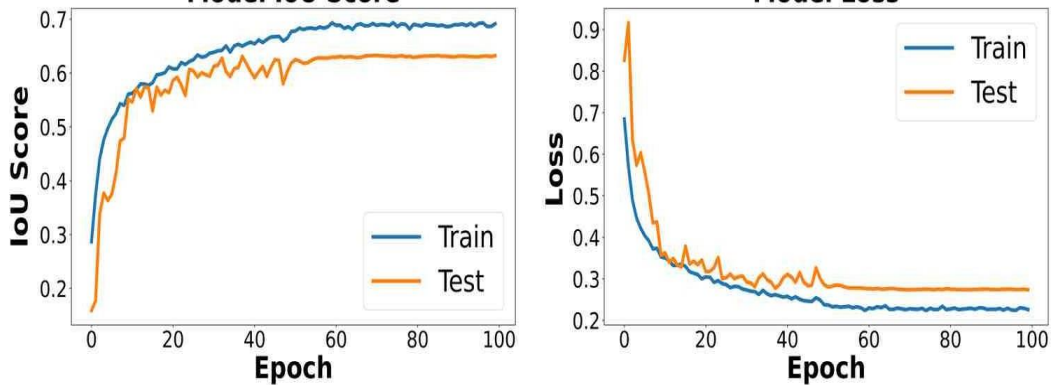
Fig 3: Prediction Scores by FPN



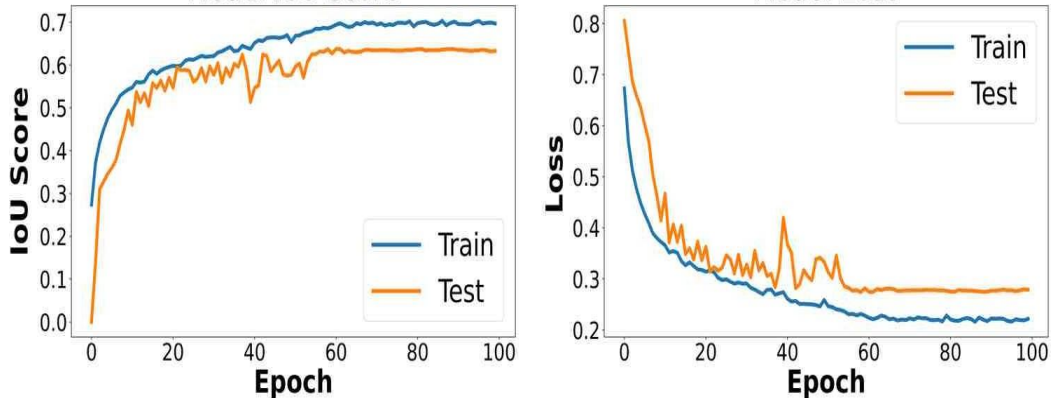
(a) Score of Prediction by PSPNet with Inception2 as backbone



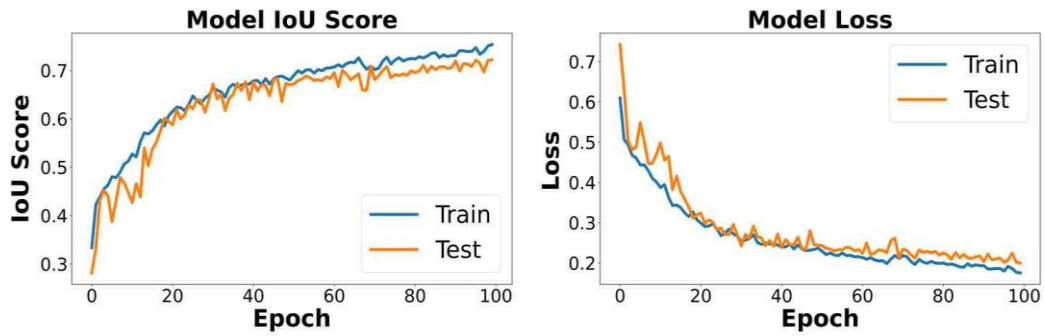
(b) Score of Prediction by PSPNet with MobileNet as backbone



(c) Score of Prediction by PSPNet with ResNet50 as backbone



(d) Score of Prediction by PSPNet with ResNet152 as backbone



(e) Score of Prediction by PSPNet with VCG19 as backbone

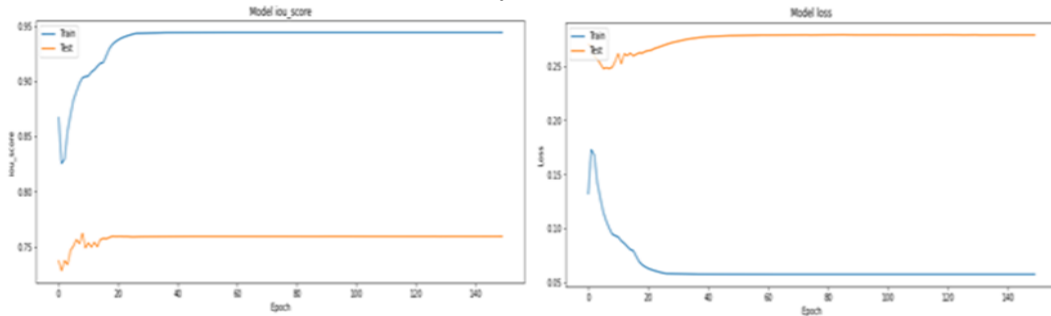


Fig 5: Score of Prediction by M-RCNN

B. Convergence Analysis

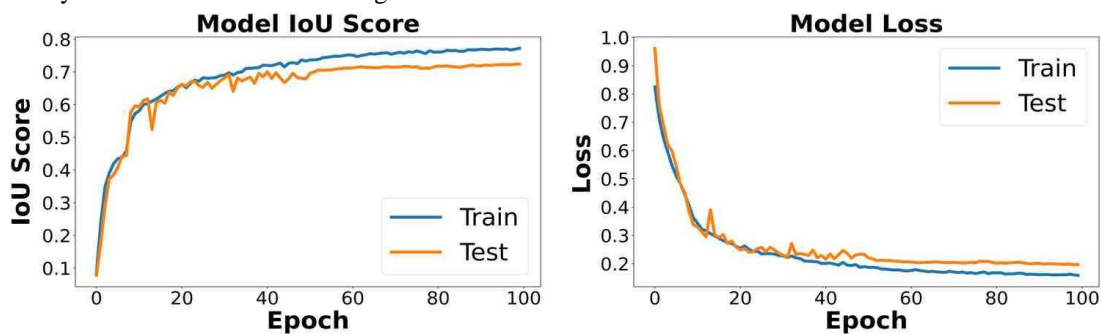
The prediction masks with our proposed technique are given in Figure 3, 4, 5 and 6. It can be seen from Figures that the top three performing model architectures are FPN with ResNet152, M-RCNN with ResNet101, and PSPNet with VGG19. This is because as we have seen that values of considered parameters for FPN are highest with ResNet152, for M-RCNN are better with ResNet101 and for PSPNet are also best with VGG19. On the other hand, the pixel accuracy, cohen’s kappa, IoU score, AuC, Recall Precision, and F1 Score of MR-CNN with ResNet101 is better compared to other backbone networks. Finally, we present the convergence analysis of our proposed technique. We show the convergence of the model architectures against each considered backbone networks. The CLAHE, Gaussian Blurr and different types of augmentation like translation, Rotation, Flipping have been done. Prediction by FPN With ResNet50, ResNet152, VGG19 as backbone FPN with ResNet152 is highest compared to all other scores. Similarly, Table 4 shows that mAP, AuC and F1 Scores for FPN with ResNet152 and VCG19 are highest respectively. Therefore, it may be concluded that the FPN gives the best

accuracy among all models proposed in this paper. The high F1 score and AuC scores for the top three models confirm that the FPN architecture performs best among all other architectures. It gives pixel accuracy above 90% for three backbones, namely ResNet152, VGG-19, and ResNet50. **MRCNN has 2 backbones due to the computational complexity over local computer**

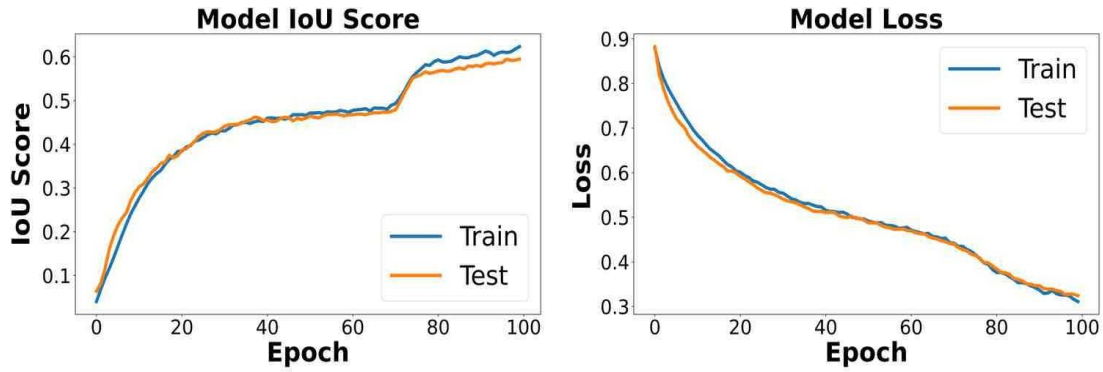
The Pixel Accuracy of 91% for LinkNet with ResNet152 is highest. The values of Recall and Precision are highest for LinkNet with ResNet50 and ResNet152 respectively.

The Pixel Accuracy with ResNet50 and Cohen’s Kappa Score and IoU Score with VGG19 for PSP-Net are better compared to other two backbone networks. The values of AuC with ResNet50, Recall with ResNet152 Precision and F1 Score with ResNet50 are best.

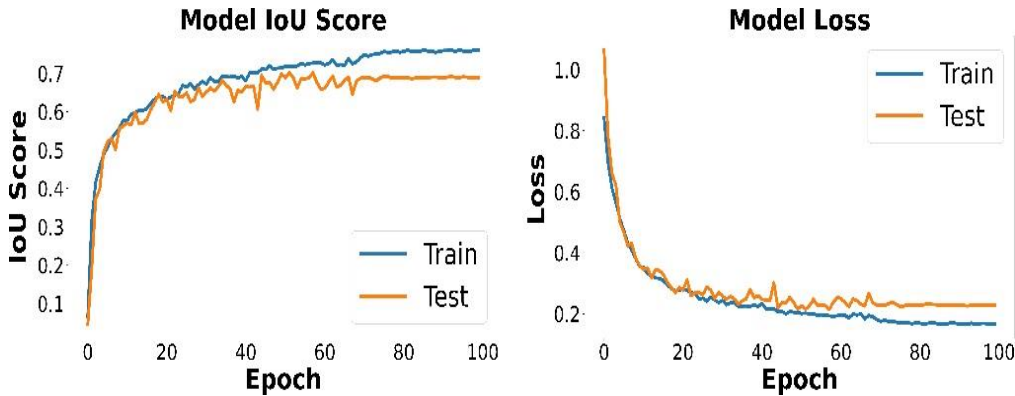
It can specifically be inferred about PSPNet that the PSPNet architecture performs well with VGG-19, ResNet50 and ResNet152 respectively as its backbone networks. We also present a graph plotting the convergence time for all model architectures against each backbone networks in Figure LinkNet has lowest precision so the prediction mask is omitted.



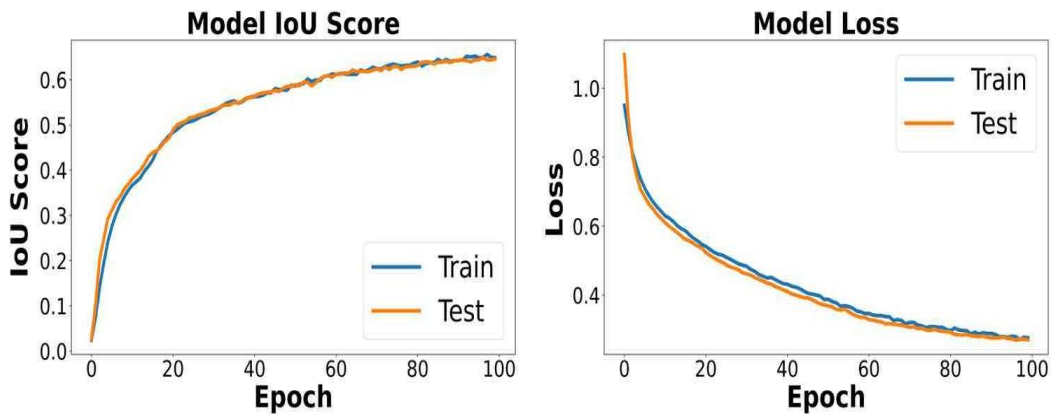
(d) Score of Prediction by LinkNet with Inception3 as backbone



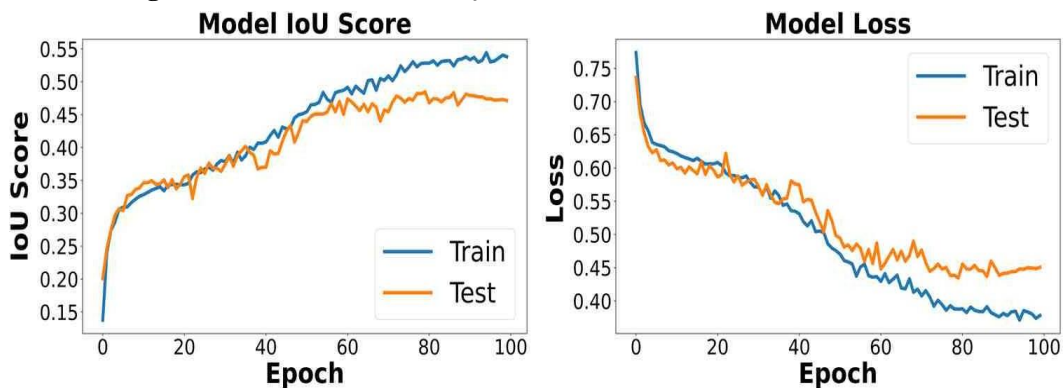
(e) Score of Prediction by LinkNet with MobileNet as backbone



(f) Score of Prediction by LinkNet with ResNet152 as backbone



(g) Score of Prediction by LinkNet with EfficientNet as backbone



(h) Score of Prediction by LinkNet with VGG19 as backbone

C. Case Study

Case study is presented considering urban images. The accuracy of prediction is shown in Figure 7, 8, and 9 in terms of mask.



Fig 7: Results of Prediction by FPN with ResNet152 backbone.



Fig 8: Results of Prediction by PSPNet



Fig 9: Results of Prediction by M-RCNN

VI. CONCLUSION

This paper presents an image segmentation and classification technique of urban cover areas using Polarimetric SAR (PolSAR) which works based on Deep Neural Networks (DNNs) such as PSPNet, LinkNet, FPN, and Mask-RCNN. Here, we first applied polarimetric decomposition on airborne Uninhabited Aerial Vehicle Synthetic Aperture (UAVSAR) images of urban areas and then the decomposed images are fed into DNNs for segmentation and classification. Four different experimentations are carried out using four different databases and models such as PSPNet, LinkNet, FPN, and Mask-RCNN and then results obtained from the experimentations are compared with different backbone networks such as ResNet152, ResNet101, ResNet50, and

VGG19. In comparison, it is seen that the FPN model with the ResNet152 as a backbone network obtained the best results on considered performance metrics such as mean Average Precision Score (mAP) and pixel accuracy. Specifically, it achieves the pixel accuracy of 90.9% and the mAP score of 0.823 and outperforms other Deep Learning models. In the future, the authors would like to explore for integrating the proposed technique for change detection and classification of multi-class objects in the domain of image processing. For few assets the MRCNN is best and for large assets FPN is the best ML tool we have been used for satellite image segmentation and classification.

ACKNOWLEDGEMENT

The authors are thankful to Shivam Aranya, Sayanati Dutta, Raisa Chaterjee, Tripti Kumari, Dr Tapan Misra, Dr Arundhati Misra Ray, Dr Rintu Kumar Gayen, Dr. Sajal Sarkar and other teachers and students to whom we care for.

DECLARATION STATEMENT

Funding	No, I did not receive.
Conflicts of Interest	No conflicts of interest to the best of our knowledge.
Ethical Approval and Consent to Participate	No, the article does not require ethical approval and consent to participate with evidence.
Availability of Data and Material	Not relevant.
Authors Contributions	All authors have equal participation in this article.

REFERENCES

- Z. Niu, G. Hua, X. Gao, et al., "Context aware topic model for scene recognition," in *2012 IEEE Conference on Computer Vision and Pattern Recognition*, 2743–2750, IEEE (2012).
- S. A. Taghanaki, K. Abhishek, J. P. Cohen, et al., "Deep semantic segmentation of natural and medical images: a review," *Artificial Intelligence Review* **54**(1), 137–178 (2021). <https://doi.org/10.1007/s10462-020-09854-1>
- T. Zhou, Z. Li, and J. Pan, "Multi-feature classification of multi-sensor satellite imagery based on dual-polarimetric sentinel-1a, landsat-8 oli, and hyperion images for urban land-cover classification," *Sensors* **18**(2), 373 (2018). <https://doi.org/10.3390/s18020373>
- S.-W. Chen and C.-S. Tao, "Polarimetric image classification using polarimetric-feature-driven deep convolutional neural network," *IEEE Geoscience and Remote Sensing Letters* **15**(4), 627–631 (2018). <https://doi.org/10.1109/LGRS.2018.2799877>
- Y. Zhang, J. Zhang, X. Zhang, et al., "Land cover classification from polarimetric sar data based on image segmentation and decision trees," *Canadian Journal of Remote Sensing* **41**(1), 40–50 (2015). <https://doi.org/10.1080/07038992.2015.1032901>
- S. De, L. Bruzzone, A. Bhattacharya, et al., "A novel technique based on deep learning and a synthetic target database for classification of urban areas in polarimetric sar data," *IEEE Journal of Selected Topics in Applied Earth Observations and Remote Sensing* **11**(1), 154–170 (2017). <https://doi.org/10.1109/JSTARS.2017.2752282>
- S. De, L. Bruzzone, A. Bhattacharya, et al., "A novel technique based on deep learning and a synthetic target database for classification of urban areas in polarimetric sar data," *IEEE Journal of Selected Topics in Applied Earth Observations and Remote Sensing* **11**(1), 154–170 (2018). <https://doi.org/10.1109/JSTARS.2017.2752282>
- Z. Cui, Q. Li, Z. Cao, et al., "Dense attention pyramid networks for multi-scale ship detection in sar images," *IEEE Transactions on Geoscience and Remote Sensing* **57**(11), 8983–8997 (2019). <https://doi.org/10.1109/TGRS.2019.2923988>
- S. Ren, K. He, R. Girshick, et al., "Faster r-cnn: Towards real-time object detection with region proposal networks," *Advances in neural information processing systems* **28**, 91–99 (2015).
- S. P. Mohanty, J. Czakon, K. A. Kaczmarek, et al., "Deep learning for understanding satellite imagery: An experimental survey," *Frontiers in Artificial Intelligence* **3**, 85 (2020). <https://doi.org/10.3389/fraci.2020.534696>
- X. Wang, L. Zhang, B. Zou, et al., "Polarimetric sar image classification based on kernel sparse representation," in *Compressive Sensing VII: From Diverse Modalities to Big Data Analytics*, **10658**, 106580L, International Society for Optics and Photonics (2018).
- A. Femin and K. Biju, "Accurate detection of buildings from satellite images using cnn," in *2020 International Conference on Electrical, Communication, and Computer Engineering (ICECCE)*, 1–5, IEEE (2020). <https://doi.org/10.1109/ICECCE49384.2020.9179232>
- X. Wang, Z. Cao, Z. Cui, et al., "Polarimetric image classification based on deep polarimetric feature and contextual information," *Journal of Applied Remote Sensing* **13**, 1 (2019). <https://doi.org/10.1117/1.JRS.13.034529>
- L. Ding, K. Zheng, D. Lin, et al., "Mp-resnet: Multipath residual

- network for the semantic segmentation of high-resolution polar images," *IEEE Geoscience and Remote Sensing Letters*, 1–5 (2021). <https://doi.org/10.1109/LGRS.2021.3079925>
- L. Zhao and E. Chen, "Segmentation and classification of polarimetric data using spectral graph partitioning," in *MIPPR 2013: Remote Sensing Image Processing, Geographic Information Systems, and Other Applications*, **8921**, 89210E, International Society for Optics and Photonics (2013). <https://doi.org/10.1117/12.2031128>
- A. Ouahabi and A. Taleb-Ahmed, "Deep learning for real-time semantic segmentation: Application in ultrasound imaging," *Pattern Recognition Letters* **144**, 27–34 (2021). <https://doi.org/10.1016/j.patrec.2021.01.010>
- Y. Chen, X. He, J. Wang, et al., "The influence of polarimetric parameters and an object-based approach on land cover classification in coastal wetlands," *Remote Sensing* **6**(12), 12575–12592 (2014). <https://doi.org/10.3390/rs61212575>
- K. He, X. Zhang, S. Ren, et al., "Deep residual learning for image recognition," in *Proceedings of the IEEE conference on computer vision and pattern recognition*, 770–778 (2016).
- S. Xie, R. Girshick, P. Dollár, et al., "Aggregated residual transformations for deep neural networks," *arXiv preprint arXiv:1611.05431* (2016). <https://doi.org/10.1109/CVPR.2017.634>
- K. Simonyan and A. Zisserman, "Very deep convolutional networks for large-scale image recognition," *arXiv preprint arXiv:1409.1556* (2014).
- P. Burlina, "Mrcnn: A stateful fast r-cnn," in *2016 23rd International Conference on Pattern Recognition (ICPR)*, 3518–3523 (2016). <https://doi.org/10.1109/ICPR.2016.7900179>
- T.-Y. Lin, P. Dollár, R. Girshick, et al., "Feature pyramid networks for object detection," in *Proceedings of the IEEE conference on computer vision and pattern recognition*, 2117–2125 (2017).
- A. Chaurasia and E. Culurciello, "Linknet: Exploiting encoder representations for efficient semantic segmentation," in *2017 IEEE Visual Communications and Image Processing (VCIP)*, 1–4, IEEE (2017). <https://doi.org/10.1109/VCIP.2017.8305148>
- H. Zhao, J. Shi, X. Qi, et al., "Pyramid scene parsing network," in *Proceedings of the IEEE conference on computer vision and pattern recognition*, 2881–2890 (2017). <https://doi.org/10.1109/CVPR.2017.660>
- S. Cloude and E. Pottier, "A review of target decomposition theorems in radar polarimetry," *IEEE Transactions on Geoscience and Remote Sensing* **34**(2), 498–518 (1996). <https://doi.org/10.1109/36.485127>
- E. Pottier and J.-S. Lee, "Application of the h/a/alpha polarimetric decomposition theorem for unsupervised classification of fully polarimetric sar data based on the wishart distribution," in *SAR workshop: CEOS Committee on Earth Observation Satellites*, **450**, 335 (2000).
- M. Neumann, L. Ferro-Famil, and E. Pottier, "A general model-based polarimetric decomposition scheme for vegetated areas," in *Proceedings of the 4th International Workshop on Science and Applications of SAR Polarimetry and Polarimetric Interferometry (ESRIN)*, Frascati, Italy, 26–30, Citeseer (2009).
- A. Freeman, "Fitting a two-component scattering model to polarimetric sar data from forests," *IEEE Transactions on Geoscience and Remote Sensing* **45**(8), 2583–2592 (2007). <https://doi.org/10.1109/TGRS.2007.897929>
- A. Freeman and S. Durden, "A three-component scattering model for polarimetric sar data," *IEEE Transactions on Geoscience and Remote Sensing* **36**(3), 963–973 (1998). <https://doi.org/10.1109/36.673687>
- J. R. Huynen, "Stokes matrix parameters and their interpretation in terms of physical target properties," in *Polarimetry: Radar, infrared, visible, ultraviolet, and X-ray*, **1317**, 195–207, International Society for Optics and Photonics (1990). <https://doi.org/10.1117/12.22083>
- A. Bhattacharya, A. Muhuri, S. De, et al., "Modifying the yamaguchi four-component decomposition scattering powers using a stochastic distance," *IEEE Journal of Selected Topics in Applied Earth Observations and Remote Sensing* **8**(7), 3497–3506 (2015). <https://doi.org/10.1109/JSTARS.2015.2420683>
- G. Singh and Y. Yamaguchi, "Model-based six-component scattering matrix power decomposition," *IEEE Transactions on Geoscience and Remote Sensing* **56**(10), 5687–5704 (2018). <https://doi.org/10.1109/TGRS.2018.2824322>



- 33 R. Barnes, "Roll-invariant decompositions for the polarization covariance matrix," in *Proceedings of the Polarimetry Technology Workshop, Redstone Arsenal, AL, USA*, **1618** (1988).
- 34 W. A. Holm and R. M. Barnes, "On radar polarization mixed target state decomposition techniques," in *Proceedings of the 1988 IEEE National Radar Conference*, 249–254, IEEE (1988).
- 35 M. Arii, J. J. van Zyl, and Y. Kim, "Adaptive model-based decomposition of polarimetric sar covariance matrices," *IEEE Transactions on Geoscience and Remote Sensing* **49**(3), 1104–1113 (2011). <https://doi.org/10.1109/TGRS.2010.2076285>
- 36 W. An, Y. Cui, and J. Yang, "Three-component model-based decomposition for polarimetric sar data," *IEEE Transactions on Geoscience and Remote Sensing* **48**(6), 2732–2739 (2010). <https://doi.org/10.1109/TGRS.2010.2041242>
- 37 W. An, C. Xie, X. Yuan, *et al.*, "Four-component decomposition of polarimetric sar images with deorientation," *IEEE Geoscience and Remote Sensing Letters* **8**(6), 1090–1094 (2011). <https://doi.org/10.1109/LGRS.2011.2157078>
- 38 Y. Yamaguchi, G. Singh, C. Yi, *et al.*, "Comparison of model-based four-component scatter- ing power decompositions," in *Conference Proceedings of 2013 Asia-Pacific Conference on Synthetic Aperture Radar (APSAR)*, 92–95, IEEE (2013).
- 39 Y. Yamaguchi, T. Moriyama, M. Ishido, *et al.*, "Four-component scattering model for po- larimetric sar image decomposition," *IEEE Transactions on Geoscience and Remote Sensing* **43**(8), 1699–1706 (2005). <https://doi.org/10.1109/TGRS.2005.852084>
- 40 E. Pottier, F. Sarti, M. Fitzryk, *et al.*, "Polsarpro-biomass edition: The new esa polarimetric sar data processing and educational toolbox for the future esa & third party fully polarimetric sar missions," in *ESA Living Planet Symposium 2019*, (2019).
- 41 B. Mr. K., Balasaram, M., Vishwanath, K. G., SK, R., & Samuel, B. J. (2020). A Dynamic Multi Label Image Classification based on Recurrent Neural Networks. In *International Journal of Recent Technology and Engineering (IJRTE)* (Vol. 8, Issue 6, pp. 5093–5096). <https://doi.org/10.35940/ijrte.f9817.038620>
- 42 Crop Detection and Classification using Remote Sensing Images. (2019). In *International Journal of Innovative Technology and Exploring Engineering* (Vol. 8, Issue 12S, pp. 1165–1173). <https://doi.org/10.35940/ijitee.k1318.10812s19>
- 43 Kumar, P., & Rawat, S. (2019). Implementing Convolutional Neural Networks for Simple Image Classification. In *International Journal of Engineering and Advanced Technology* (Vol. 9, Issue 2, pp. 3616–3619). <https://doi.org/10.35940/ijeat.b3279.129219>

AUTHORS PROFILE



Tamesh Halder, Department of Mining Engineering Indian Institute of Technology Kharagpur, India Unmanned Aerial Vehicles, Synthetic Aperture Radar, Ad Hoc Networks, Agroforestry, Digital Elevation Model, Extreme Learning Machine, Flying Ad Hoc Networks, Global Positioning System, Path Loss, Point Cloud, Point Cloud Model, Polarimetric Synthetic Aperture Radar, Receiver Operating

Characteristic Curve, 3D Mesh, Acid Mine Drainage, Acquisition Unit, Adaptive Algorithm, Adaptive Filter, Additive Noise, Aerial Images, Aerodynamic, Agisoft Photo Scan, Area Under Curve, Artifact Removal, Atmospheric Oxygen Tamesh Halder received the B.Tech. degree in electronics and instrumentation engineering from the University of Kalyani in 2010, and the M.S. degree in electronics and electrical communications engineering from the Indian Institute of Technology Kharagpur, Kharagpur, in 2013, where he is currently pursuing the Ph.D. degree with the Department of Mining Engineering. His research experience includes remote sensing, focal source localization, compressive sensing, beamformers, receiver operating characteristics, EEG, MEG, and machine learning.



Soumyadip Sarkar, Activities: ex- ML intern @IIT Kharagpur | Junior ML researcher at IEDC Lab | Kaggle Kernel Expert | Deep Learning | Computer Vision | NLP | Love Python and C++ Summary: Hello, it's Soumyadip Sarkar, in 2022 pass out from Electrical Engineering, IEM Kolkata, India. I have experience in Computer Vision, NLP, Machine Learning, Deep Learning. I am familiar with backend

development for ML/DL models using flask and streamlit and Docker. I love participating in Kaggle competitions and different Hackathons. I also like doing Open-Source Contributions and writing blogs. Performed

different qualitative and quantitative experiments on Mask RCNN model for image segmentation of PolSAR data.



Farhan Hai Khan, ML Head at Applex.in | Jr. ML Researcher at IEM IEDC | Kaggle Expert | ex-ML Intern IIT KGP | ex-Data Science Intern BrickView Studios | WoC 20 and GSSoC 21 Mentor | AI Team @DSC-IEM | Core IET IEM | IEM EE Hello, this is Farhan Hai Khan my bachelors degree in Electrical Engineering from Institute of Engineering and Management, Kolkata at 2022. I'm a Machine Learning enthusiast, also good at Algorithms Design, and Project Work. Developing Deep Learning skills this year. Work done during the internship period: Polarimetric Orientation Angle Estimation using various Stochastic Distancing Techniques .Hellinger, Renyi of Order Beta, Wasserstein, Bhattacharya Distances. Remote Sensing based GeoData.



Shobhit Kumar, Activities: ex-Summer intern at Tata steel(Tech Team), Ex-Research intern @iit kharagpur || CP(3) @codechef||Data Science from IIT Madras || ML enthusiast||DevOps Hello, it's Shobhit Kumar, studied at IEM Kolkata, India since Nov 2020 pursuing B.Tech at computer science . I have experience in Computer Vision, NLP, Machine Learning, Deep Learning.



Dipjyoti Paul, Affiliation Department of Computer Science, University of Crete, Rethymno, Greece, Publication Topics, Generative Adversarial Networks, Convolutional Layers, Fréchet Inception Distance, Generative Adversarial Networks Training, Nash Equilibrium, Neural Network, Adult Male, Baseline Training, Batch Normalization, Convergence Rate, Covariance Matrix, Deep Neural Network, F-statistic, Gaussian Mixture Model, Generative Adversarial Networks Loss, Generator Training, Hellinger Distance, High-quality, Higher-order Statistics, Hourly Data, Hyperparameter Values, Image Generation, Inception Distance, Kullback-Leibler, Learning Rate Dipjyoti Paul received the B.Tech. degree in electronics and communication engineering from the St. Thomas' College of Engineering and Technology under the West Bengal University of Technology, Kolkata, India, in 2013, and the M.Sc. degree in electronics and electrical communication engineering from the Indian Institute of Technology Kharagpur (IIT Kharagpur), Kharagpur, India, in 2017. He is currently pursuing the Ph.D. degree in speech signal processing with the Department of Computer Science, University of Crete, Rethymno, Greece. His research interests include diverse areas, such as machine/deep learning, signal/speech processing, computer vision, and optimization theory. He also has a broad interest in probabilistic machine learning methods and generative models. Mr. Paul is also a member of ISCA.



Debashish Chakravarty, Affiliation Mining Engineering Indian Institute of Technology Kharagpur Kharagpur, India Publication Topics Unmanned Aerial Vehicles, Global Positioning System, Synthetic Aperture Radar, Ad Hoc Networks, Agroforestry, Convolutional Neural Network, Digital Elevation Model, EEG Data, Extreme Learning Machine, Flying Ad Hoc

Networks, Land Use, Land Use/land Cover, Machine Learning, Mining Regions, Normalized Difference Vegetation Index, Path Loss, Performance Metrics, Point Cloud, Point Cloud Model, Polarimetric Synthetic Aperture Radar, Receiver Operating Characteristic Curve, Water Bodies, 3D Mesh, Acid Mine Drainage, Acquisition Unit Debashish Chakravarty received the B.Tech. and M.Tech. degrees in mining engineering, the Ph.D. degree from the Indian Institute of Technology Kharagpur, Kharagpur, in 1998, and the Postdoctoral degree in applied mathematics and computer science from BAT, Germany, in 2003. He is an Associate Professor with the Department of Mining Engineering, Indian Institute of Technology Kharagpur. He is the Professor-in-Charge of the Autonomous Ground Vehicle Students' Research Group. He is also associated with the Advanced Technology Development Centre, Indian Institute of Technology Kharagpur. His areas of research are remote sensing, rock mechanics, numerical models

Disclaimer/Publisher's Note: The statements, opinions and data contained in all publications are solely those of the individual author(s) and contributor(s) and not of the Blue Eyes Intelligence Engineering and Sciences Publication (BEIESP)/ journal and/or the editor(s). The Blue Eyes Intelligence Engineering and Sciences Publication (BEIESP) and/or the editor(s) disclaim responsibility for any injury to people or property resulting from any ideas, methods, instructions or products referred to in the content.